*International Journal of Microwave and Wireless Technologies*, 2012, 4(1), 101–107. 
doi:10.1017/S175907871100095X

RESEARCH PAPER

# Generation of electrical self-oscillations in two-terminal switching devices based on the insulator-to-metal phase transition of $VO_2$ thin films

JONATHAN LEROY[1], AURELIAN CRUNTEANU[1], JULIEN GIVERNAUD[1], JEAN-CHRISTOPHE ORLIANGES[2], CORINNE CHAMPEAUX[2] AND PIERRE BLONDY[1]

*We present the non-linear electrical properties of simple two-terminal switching devices based on vanadium dioxide ($VO_2$) thin films. The current–voltage characteristics of such devices present negative differential resistance (NDR) regions allowing generating electrical self-oscillations across the investigated devices, with frequencies ranging from several kHz up to 1 MHz. We investigate and compare the factors determining the onset of oscillatory phenomenon in both voltage- and current-activated oscillations and explain its origin. For both activation modes, we will correlate the properties of electrical oscillations (amplitude and frequency) with the amplitude of the continuous excitation signal, the physical geometry of the devices or ambient temperature. We conclude by mentioning several possible applications for the oscillation generation in the radiofrequency (RF)/microwave domains (inverters, integrated a.c. signal generators, pressure and temperature sensors, etc.).*

**Keywords:** Vanadium dioxide, Electrical switching, Self-oscillations, Metal-insulator transition

Received 30 May 2011; Revised 19 September 2011; first published online 17 November 2011

## I. INTRODUCTION

Currently, smart materials are the subject of increasing attention for the scientific community because of their ability to change their properties (resistivity, dielectric, magnetic, optical constants, etc.) under external stimuli, which makes them potential attractive candidates for a broad range of applications where tunable devices and systems are needed [1]. Among these materials, the vanadium dioxide ($VO_2$) is an interesting system to be studied, since it presents a reversible, temperature-induced metal–insulator transition (MIT) at 68°C, transition that induces major changes in its electrical and optical properties [2, 3]. Thus, at room temperature, $VO_2$ has the properties of a semiconductor with monoclinic crystal structure but above its transition temperature of 68°C, the material behaves like a metal, with a rutile tetragonal structure. Consequently, this electronic and structural transition is accompanied by a significant change in the electrical resistivity of the material (three to five orders of magnitude) and modifies consequently its optical and tribological properties [2, 3]. More interesting, besides the thermal-induced transition [2, 4], the MIT of $VO_2$ thin films can be triggered on faster timescales (picoseconds to nanoseconds) using different stimuli: electron injection (voltage- or current-induced MIT) [3, 4], optically (photon absorption) [5], or under the effect of an external stress [6]. The electrically triggered MIT-inducing resistivity change of $VO_2$-based two-terminal (2 T) devices was already used to demonstrate electrical switches from DC to microwave [7], and THz frequencies [8], integrated reconfigurable filters in the microwave domain [9, 10] or microwave power limiters [11].

Recently, several reports [4, 12] highlighted the non-linear *I–V* characteristic of electrical switches based on $VO_2$ thin layers and the occurrence of periodic signals (self-oscillations) maintained across 2 T devices. The phenomenon is initiated by applying a continuous voltage to the 2 T device (carrier injection).

In this paper, we demonstrate the appearance of similar self-oscillations across $VO_2$-based 2 T devices in the case of continuous or pulsed current injection in the devices. We will show that this current activation scheme generating self-oscillations across the device has several advantages compared to the voltage-activated oscillations and we will try to establish a physical model explaining its appearance in the non-linear device. We will also compare the properties and the conditions for self-oscillation generation in the $VO_2$-based 2 T devices for both current- and voltage-activated phenomena.

## II. EXPERIMENTAL

The 2 T $VO_2$-based electrical devices were fabricated in a similar way as presented in [7, 13]. Briefly, $VO_2$ thin films

[1]XLIM UMR 6172, CNRS/Université de Limoges, Avenue Albert Thomas, 87060 Limoges, France. Phone: +33 5 87 50 67 41.
[2]SPCTS UMR 6638, CNRS/Université de Limoges, CEC, 12 rue Atlantis, 87068 Limoges, France.
**Corresponding authors:**
J. Leroy and A. Crunteanu
Emails: jonathan.leroy@xlim.fr; aurelian.crunteanu@xlim.fr

were deposited on C-type sapphire substrates using reactive laser ablation of a pure vanadium target (99.95%) in an oxygen atmosphere (the experimental conditions are detailed elsewhere [9]). The obtained films, with thicknesses up to 200 nm, are crystalline and show a resistivity change of four to five orders of magnitude during the thermally initiated MIT [11]. The 2 T electrical switches were manufactured in clean room environment [9, 11] using conventional microfabrication techniques. We prepared rectangular patterns of $VO_2$ (defined by optical lithography and wet etching) on which we deposit a pair of metallic electrodes (Cr/Au bi-layer) separated by different distances. The distance between the metallic electrodes defines the length of the $VO_2$ device [13]. We investigated devices with different lengths from 5 μm up to 350 μm.

The current–voltage (*I–V*) characteristics of the obtained 2 T devices is recorded by introducing the device into a simple electrical circuit (insert in Fig. 1(a)), containing a series resistance, $R_S$ (typical 1 kΩ), and a source meter (Keithley 2612A) operating in both voltage and current modes. The source provides power to the circuit and allows measuring the circuit current and the voltage across its terminals. For studying the appearance of the oscillation regime, we measured the voltages across all the circuit elements ($VO_2$ device and series resistance) using a broad bandwidth four-channel oscilloscope (Tektronix DPO7254): the first channel was used to measure the voltage across the $VO_2$ device, while the second one monitors the current flowing in the circuit (through the voltage drop in the series resistor).

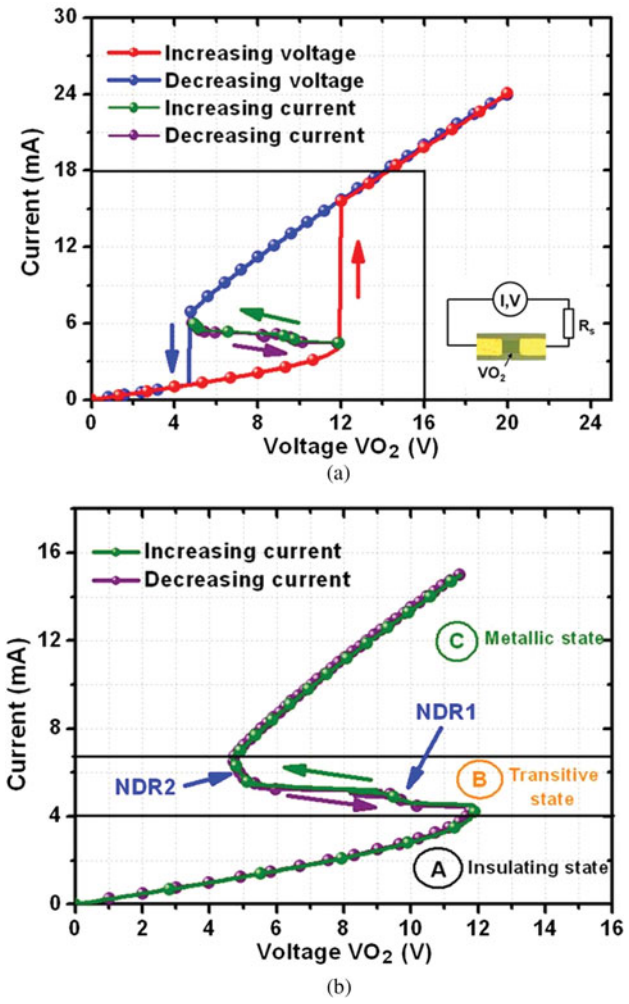


**Fig. 1.** (a) *I–V* characteristic in voltage- and current-mode of a device incorporating a $VO_2$ pattern (25-μm-long and 18-μm-wide) within insert, the test circuit; (b) zoom on the *I–V* characteristic of the current mode.

## III. RESULTS AND DISCUSSION

### A) Non-linear *I–V* characteristic of $VO_2$-based devices

A typical *I–V* characteristic of a 2 T $VO_2$-based switch ($VO_2$ pattern of 25 μm in length and 18 μm in width) is shown in Fig. 1(a) for both voltage and current modes. The MIT electrically induced MIT transition is clearly visible for both activation modes as an abrupt change in the device's resistance, marked by a sudden increase of current in the circuit for $V_{th} \sim 12$ V in the voltage mode (indicated by an arrow, red curve) or by a sudden decrease of the switch voltage in the current mode, for injected currents of $I_{th} \sim 4$ mA. In the voltage-activated MIT mode, the transition presents an important hysteresis loop (when sweeping back the voltage), associated probably with thermal effects developed in the device due to "jumping" toward high current values after the MIT. This hysteretic behavior becomes practically inexistent during the current-activated MIT (almost perfect superposition of the two upward and downward current-sweeping curves, see Fig. 1(a)). For both types of electrical activation, one can identify three main regions in the *I–V* characteristic, as indicated in Fig. 1(b) for the current-activated transition: the first region (A), of low currents (between 0 and ~4 mA for the investigated device), corresponding to a highly resistive, semi-conducting state for the $VO_2$ layers, the second, highly non-linear region (B) related to the MIT transition of the material and, finally, the third zone (C) corresponding to a low resistance state of the $VO_2$, when the material changes to its metallic state (strong currents, above 15 mA). As indicated in Fig. 1(b), the non-linear region (B) (in the current mode) shows two sub-regions presenting negative differential resistance (NDR1 and NDR2). It was suggested that the emergence of these NDR regions is the result of a progressive apparition of the MIT in the $VO_2$ material, in a percolative manner (gradual growth of metallic $VO_2$ nano-domains within the $VO_2$ semiconductor matrix and co-existence between the semi-conductor and metallic domains in the $VO_2$ films) [6, 14, 15]. Similar 2 T $VO_2$ circuits integrated on coplanar waveguides were previously extensively studied in the RF/microwave domains [7, 9–11] and besides their employment as broadband, high-speed microwave switches, they show potential to sustain RF powers levels up to several watts, depending on their geometry and type of implementation (shunt or series configurations) [11].

### B) Current-induced self-oscillations in the $VO_2$ switches

It is well known that the presence of an NDR region in a component *I–V* characteristic is one of the prerequisite properties for obtaining current/voltage oscillations [16, 17]. To verify this and for initiating the oscillating phenomenon in the current mode, we applied in the electrical circuit (insert in

https://doi.org/10.1017/S175907871100095X Published online by Cambridge University Press

Fig. 1(a)) square-type current signals (2-ms long) with different amplitudes that corresponds to the different regions (A, B-NDR1 and B-NDR2 and C) in the *I–V* characteristic of the 25 μm × 18 μm $VO_2$ device.

As illustrated in Fig. 2, we observed the apparition of the current-induced self-oscillations in the $VO_2$ material only for current amplitudes corresponding to the first NDR region (NDR1). Thus, the origin of these oscillations is directly related to the presence of the NDR region in the *I–V* characteristic of the device operated in the current mode.

Figure 3 shows the typical shape of the voltage oscillation over a period for both the voltage across the $VO_2$ device (red curve) and the voltage across the series resistance (blue curve) (for a 350-μm-long and 50-μm-wide device, heated to 50°C). The shape of the $VO_2$ voltage curve suggests behavior similar to a relaxation oscillator: a capacitance (the $VO_2$ material, seen as a percolative mixture of metallic and isolating nano-domains) is charging until the electrical field across it reaches a critical value (zone (E) in Fig. 3). For certain materials, this critical field may cause the destruction of the material because it corresponds to the maximum electrical field that the material can handle (disruptive or electrical breakdown field). In the case of $VO_2$, this threshold electrical field will trigger the MIT transition and the material changes abruptly to a low-resistance metallic state, leading to the formation of a highly conductive path between the two metallic electrodes (zone (F) in Fig. 3). The charges accumulated on the electrodes of the device are rapidly released in the circuit and a current pulse is created (corresponding to the voltage pulse on the series resistor, blue curve in Fig. 3). The electric field across the $VO_2$ switch drops sharply to values corresponding to the $VO_2$'s isolating state and the material recovers its original semiconductor state and, if the conditions for the onset of oscillating behavior are satisfied, a new cycle of oscillations begins. During one period of oscillation (zones (E) and (F) in Fig. 3), the shape of the $VO_2$ voltage-charging curve (before the initiation of the MIT) can be fitted (equivalent to several constants) with a well-known expression derived from an RC circuit analysis:

$$V_{VO_2} \sim V_{ap}(1 - \exp(-t/t), \quad (1)$$

where $V_{ap}$ is the overall delivered voltage by the source meter and $\tau = RC_T$ is the time constant of the circuit, as the product of the overall resistance in the circuit ($R_S + R_{VO_2}$) and of its overall capacitance, $C_T$.

The equivalent circuit of the $VO_2$ 2 T switch (in the electrical diagram in the inset in Fig. 1(a)) can be represented as a variable capacitor, $C_{VO_2}$, in parallel with a variable resistor, $R_{VO_2}$, both of which are functions of the voltage across the device (but also of the ambient temperature as for the thermally triggered MIT [2–4, 7]). Most likely, the shape of the $VO_2$ voltage-charging curve during oscillations in the zone (E) in Fig. 3 is governed by the overall capacitance ($C_T$) of the electrical circuit depicted in the inset in Fig. 1(a). This overall capacitance includes, besides the variable capacitance $C_{VO_2}$, also a small contribution from parasitic capacitances coming from connecting cables. To verify the influence of external capacitances in the circuit, we included, in parallel to the $VO_2$ switch, additional capacitors with precise capacitance values ($C_P$). Preliminary results (experiments are still underway) show that, in these cases, the self-oscillation frequencies decrease with increase in the added capacitances values. The phenomenon can be explained by an increase in the overall capacitance of the circuit ($C_P$ and $C_{VO_2}$ will add, since in parallel) and, consequently, of the time constant in the circuit ($\tau = RC_T$), which involves a decrease in the oscillating frequencies.

The self-oscillation frequency appearing in the NDR1 varies between 1 kHz and 1 MHz, depending primarily not only on the size of the $VO_2$ pattern but also on excitation or external environmental parameters (temperature) as will be shown in Section III(D).

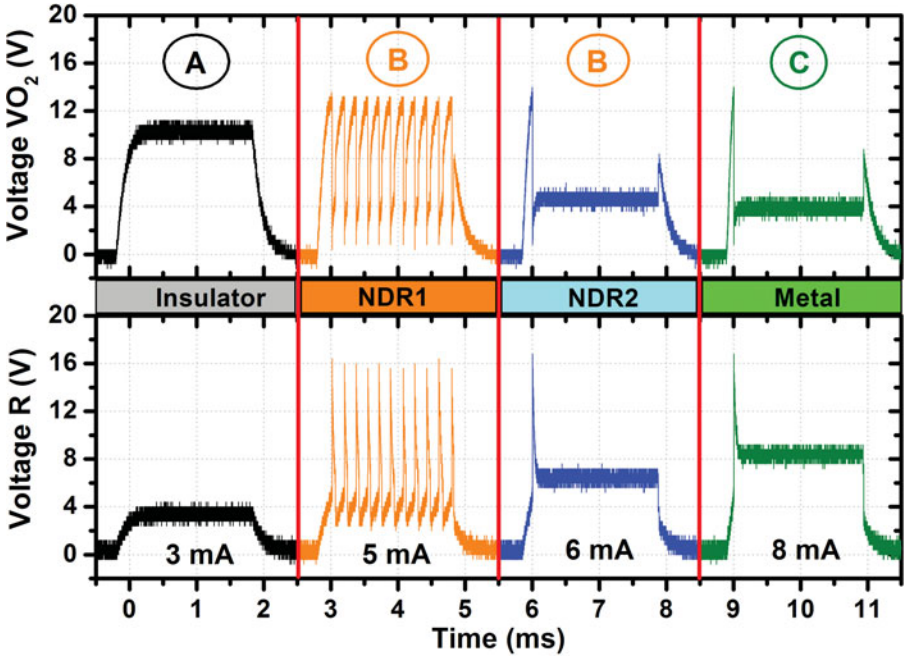


**Fig. 2.** Voltage pulses observed across of $VO_2$ pattern and series resistance during the injection of current pulses of 2 ms with different amplitudes in the device of Fig. 1.

https://doi.org/10.1017/S175907871100095X Published online by Cambridge University Press

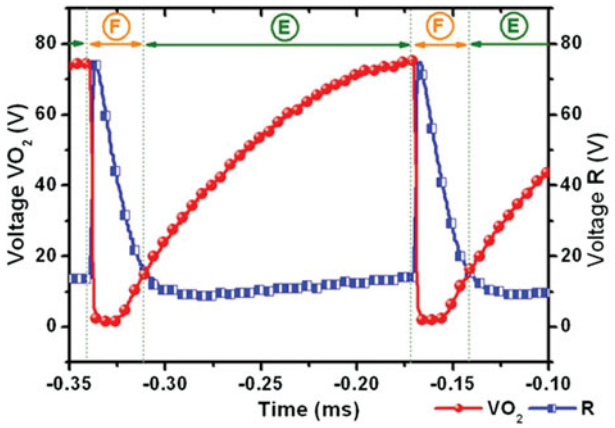


**Fig. 3.** Evolution of the voltage across the pattern of $VO_2$ (round symbols) and across the series resistance (squared symbols) during a period of oscillation for a device incorporating a $VO_2$ pattern of 350-μm-long and 50-μm-wide, heated to 50°C.

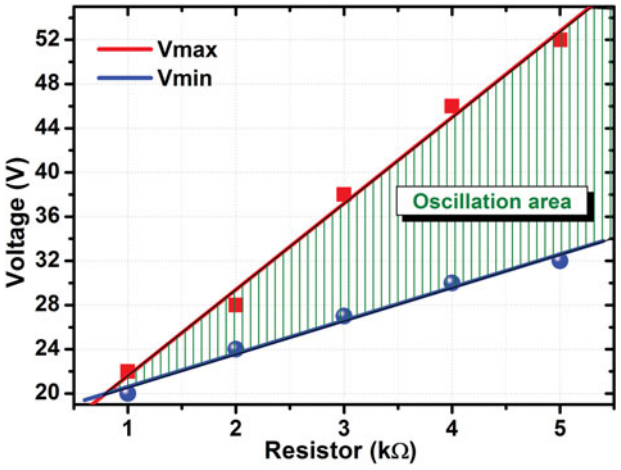


**Fig. 4.** Evolution of the voltage range where oscillations are observed as a function of the series resistance on a device with a $VO_2$ pattern 25 × 18 μm².

Regarding the second NDR region (NDR2) of the device *I*–*V* characteristic, for the excitation circuit we used, we were not able to identify the onset of electrical oscillations. A possible explanation is that this NDR2 is not intrinsic to the $VO_2$ material as is the NDR1, but rather is circuit dependent. When increasing the current along the *I*–*V* characteristic, at the end of the NDR1, the component has a negative resistance that largely compensates that of the series resistance, $R_S$. Further increasing the current will decrease (in absolute value) this negative resistance until the point where $R_S$ will become larger (at the end of NDR2). After this point, the component will enter an ohmic regime (metallic region in Fig. 1(b)). However, it is possible to initiate oscillations also in this NDR2 zone, by integrating in the excitation circuit additional elements (*R*, *C*, and *L* components).

## C) Voltage-induced self-oscillations in the $VO_2$ devices

In the voltage-excitation mode, the oscillatory phenomenon seems more difficult to initiate although the oscillating mechanism is the same as for the current mode. As already demonstrated [4, 12], the appearance of the oscillating phenomenon is conditioned by specific ranges of excitation voltage and series resistance in the circuit, as shown in Fig. 4. In agreement with previous results [4, 12], we obtained a specific "window" in the applied voltage series resistance diagram for which the onset of the self-oscillating phenomenon is possible. The properties and the shape of the oscillations are similar to those obtained for the current-activation mode. We note that the oscillations do not occur for low series resistances, $R_S$, but only for specific values. In fact, the couple "applied voltage"–"series resistance" defines a load-line in the circuit which, if properly chosen, will intercept the *I*–*V* characteristics at current values corresponding to the NDR1 and thus, initiating the self-oscillating mechanism.

## D) Self-oscillation's amplitude and frequency dependence on excitation parameters

We investigated the influence of the excitation amplitude (for both current- or voltage-activation modes) on the amplitude and frequency of the self-oscillating phenomenon appearing across the $VO_2$-based devices. The two graphs in Fig. 5 show that for both activation modes, an increase in the excitation current or voltage (in the limits imposed by the NDR1) results in an increase in the oscillation frequencies and slightly reduces their amplitudes. In both cases, these

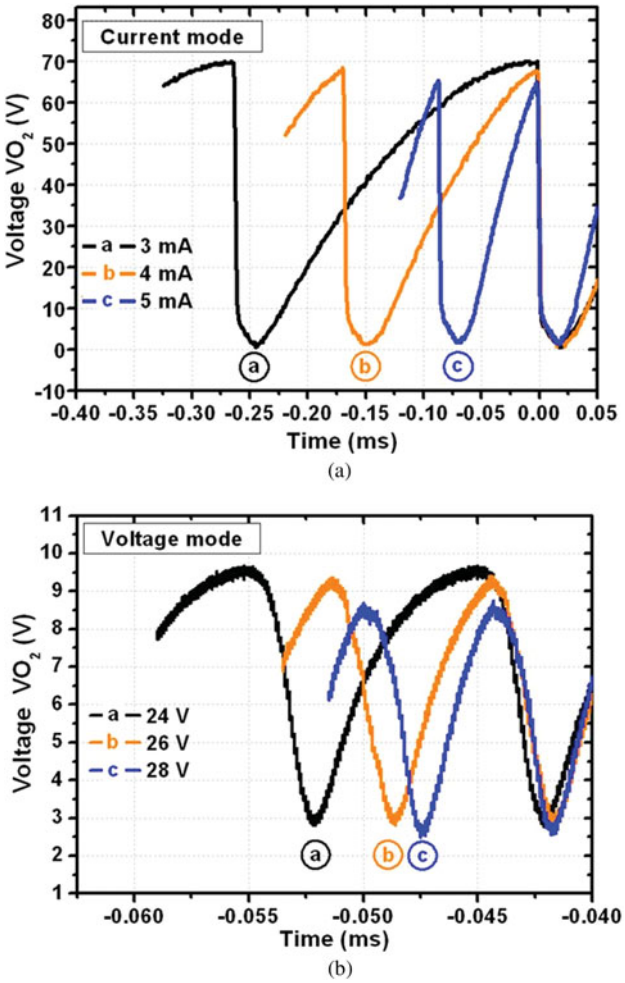


**Fig. 5.** (a) Self-oscillations observed during the application of DC currents of different values in the NDR1 of the *I*–*V* characteristic of a device with a $VO_2$ pattern of 350 × 50 μm² and (b) self-oscillations observed for different voltage values for a $VO_2$ pattern of 25 × 18 μm².

https://doi.org/10.1017/S175907871100095X Published online by Cambridge University Press

variations can be explained by the percolative mechanism responsible for the onset of self-oscillations: if the applied voltage or current increases, the proportion of metallic domains within the insulating material increases causing a decrease in the device resistivity and possibly in its overall capacitance. Since the oscillating phenomenon is governed by an RC-type time constant (the rising part of the $VO_2$ voltage oscillations), the frequency will decrease with decrease in the time constant $\tau = RC$.

Another important parameter affecting the oscillations properties is the device temperature. Increasing the temperature of the $VO_2$ device will result in an increase in the oscillation frequencies and in a more marked decrease of their amplitudes for both current- and voltage-induced oscillations (Figs 6(a) and 6(b), respectively). This behavior can be simply explained by a decrease of the initial device resistivity with temperature (the initial $\tau = RC$ time constant decreasing consequently with the temperature). It is also worth noting that above 68°C (temperature transition of the $VO_2$ material), no oscillating phenomenon occurs, since the material is totally transformed to its metallic state and its $I$–$V$ characteristic is typical of a resistance (ohmic type).

The impact of the series resistances in the excitation circuit on the characteristics of the oscillations was also investigated, for both excitation modes. In the case of current-induced self-oscillations $R_S$ has little impact on the oscillation frequencies

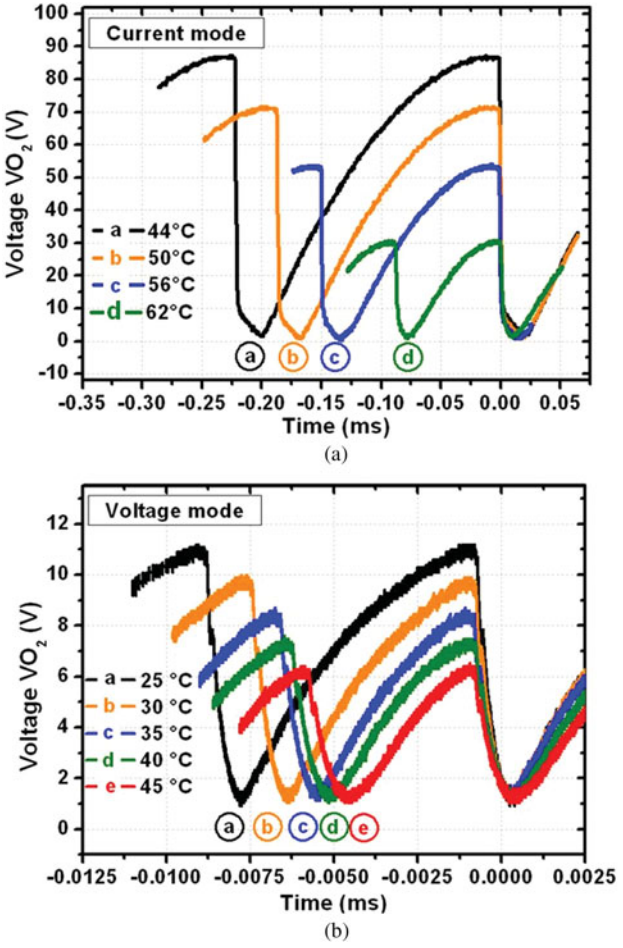


**Fig. 6.** (a) Self-oscillations observed in a device with a $VO_2$ pattern of 350 × 50 μm² for different temperatures in the case of a DC current (3 mA) and (b) in the case of a voltage of 35 V on a $VO_2$ pattern of 25 × 18 μm².

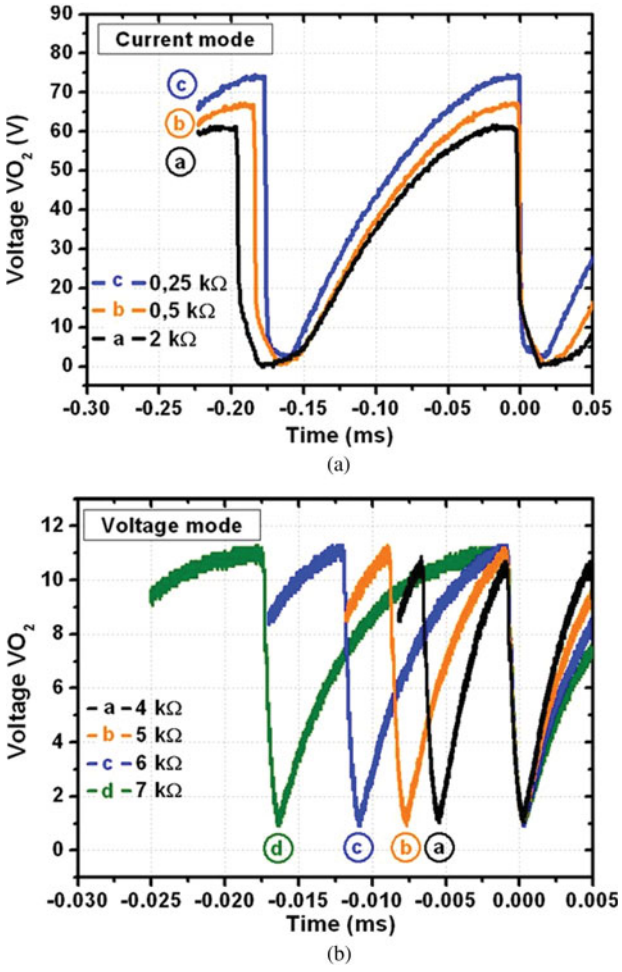


**Fig. 7.** (a) Self-oscillations observed in a device incorporating a $VO_2$ pattern of 350 × 50 μm² for different values of resistance during the application of a DC current of and (b) in the case of a voltage of 35 V on a $VO_2$ pattern of 25 × 18 μm².

and affects moderately the oscillations amplitudes (Fig. 7(a)): the frequencies are slightly increased and the amplitude tends to increase as $R_S$ grows stronger. Instead, for the voltage-induced self-oscillations mode, the increase in the values of the series resistance will slightly reduce the oscillations amplitudes but will strongly affect the frequencies of oscillations, decreasing them. It is relatively difficult to explain this phenomenon for the voltage-activated mode, but intuitively, a modification of the $R_S$ (within the limits imposed by the oscillation window shown in Fig. 4) will affect the way the load-line (applied voltage-series resistance) excites the NDR region of the device.

## IV. CONCLUSIONS

In conclusion, we demonstrated electrical self-oscillations generation in simple 2 T $VO_2$-based devices using their NDR properties, in both current- or voltage-activated modes. The physical mechanism explaining the onset of the oscillating phenomenon can be explained by the dynamic percolative occurrence of metallic and isolating nano-domains within the $VO_2$ material during excitation which makes the device behave like a charging capacitor. We demonstrated that, for both excitation modes, the oscillation amplitude

https://doi.org/10.1017/S175907871100095X Published online by Cambridge University Press

and frequencies can be controlled by the values of the continuous excitation signal, the circuit parameters, the geometrical parameters of the devices, and by external parameters such as temperature. Work is in progress for expanding the oscillation frequencies of the presented devices toward higher values (in the RF/microwave frequency domains) by coupling them with external RLC (resistance-inductance-capacitance) resonators or designing in-plane metal-insulator-metal (MIM)-type devices. The results presented here can provide simple, innovative solution for applications in the oxide electronics field: on-chip, highly integrated inverters and on-chip oscillators, a.c. signal generators for integrated nano-devices, extremely sensitive pressure/position and temperature sensors, etc.

## ACKNOWLEDGEMENT

This work was supported by the ANR France under project "Admos-VO2", ANR 07-JCJC-0047.

## REFERENCES

[1] Gevorgian, S.: Tuneable materials for agile microwave devices, in 38th European Microwave Conf., Amsterdam, The Netherlands, 2008, paper WWE6-6, 1–34.

[2] Morin, F.J.: Oxides which show a metal-to-insulator transition at the Neel temperature. Phys. Rev. Lett., **3** (1959), 34–36.

[3] Stefanovich, G.; Pergament, A.; Stefanovich, D.: Electrical switching and Mott transition in $VO_2$ 2000. J. Phys.: Condens. Matter., **12** (2000), 8837–8845.

[4] Kim, H.T. et al.: Electrical oscillations induced by the metal-insulator transition in $VO_2$. J. Appl. Phys., **107** (2010), 023702.

[5] Cavalleri, A. et al.: Femtosecond structural dynamics in $VO_2$ during an ultrafast solid-solid phase transition. Phys. Rev. Lett., **87** (2001), 237401.

[6] Kikuzuki, T.; Lippmaa, M.: Metal-insulator transition characteristics of $VO_2$ thin films grown on Ge(100) single crystals. Appl. Phys. Lett., **96** (2010), 132107.

[7] Dumas-Bouchiat, F.; Champeaux, C.; Catherinot, A.; Crunteanu, A.; Blondy, P.: RF-microwave switches based on reversible semiconductor-metal transitionof the $VO_2$ thin films synthesized by pulsed-laser deposition. Appl. Phys. Lett., **91** (2007), 223505.

[8] Choi, S.B. et al.: Nanopattern enabled terahertz all-optical switching on vanadium dioxide thin film. Appl. Phys. Lett., **98** (2011), 071105.

[9] Dumas-Bouchiat, F.; Champeaux, C.; Catherinot, A.; Givernaud, J.; Crunteanu, A.; Blondy, P.: RF microwave switches based on reversible metal-semiconductor transition properties of $VO_2$ thin films: an attractive way to realise simple RF microelectronic devices, in materials and devices for smart systems III, in *Mater. Res. Soc. Symp. Proc.* vol. 1129, Warrendale, PA, 2009, 275–286.

[10] Bouyge, D. et al.: Reconfigurable bandpass filter based on split ring resonators and vanadium dioxide ($VO_2$) microwave switches, in Asia-Pacific Microwave Conf., Singapore, 2009, 2332–2335.

[11] Givernaud, J. et al.: Microwave power limiting devices based on the semiconductor–metal transition in vanadium-dioxide thin films. IEEE Trans. Microw. Theory Tech., **58** (2010), 2352–2361.

[12] Sakai, J.: High-efficiency voltage oscillation in VO2 planer-type junctions with infinite negative differential resistance. J. Appl. Phys., **103** (2008), 103708.

[13] Crunteanu, A. et al.: Voltage- and current-activated metal-insulator transition in VO2-based electrical switches: a lifetime operation analysis. Sci. Technol. Adv. Mater., **11** (2010), 065002 (6pp).

[14] Chang, Y.J. et al.: Phase coexistence in the metal–insulator transition of a $VO_2$ thin films. Thin Solid Films, **486** (2005), 46–49.

[15] Rozen, J.; Lopez, R.; Haglund, R.F.; Feldman, L.C.: Two-dimensional current percolation in nanocrystalline vanadium dioxide films. Appl. Phys. Lett., **88** (2006), 081902.

[16] Kishida, H.; Ito, T.; Nakamura, A.; Takaishi, S.; Yamashita, M.: Current oscillation originating from negative differential resistance in one-dimensional halogen-bridged nickel compounds. J. Appl. Phys., **106** (2009), 016106.

[17] Mori, T.; Bando, Y.; Kawamoto, T.; Terasaki, I.; Takimiya, K.; Otsubo, T.: Giant nonlinear conductivity and spontaneous current oscillation in an incommensurate organic superconductor. Phys. Rev. Lett., **100**, (2008), 037001.

**Jonathan Leroy** received the Master's degree in electronics from the University of Limoges, Limoges, France, in 2010. He is currently working toward obtaining his Ph.D. at the University of Limoges. Since 2010, he is with the XLIM Research Institute, CNRS/University of Limoges. His research interests include the study of smart materials (mainly $VO_2$) and their applications in RF/microwave and THz devices.

**Aurelian Crunteanu** received the Phys. Eng. Degree in optics and optical technologies, Master's degree, and Ph.D. degree in physics from the University of Bucharest, Bucharest, Romania, in 1995, 1996, and 2000, respectively, and the Ph.D. degree in material sciences from the Claude Bernard University, Lyon 1, France, in 2001. From 2001 to 2003, as a Post-Doctoral Fellow with the Institute of Imaging and Applied Optics, Swiss Federal Institute of Technology, Lausanne, Switzerland, his research was oriented to the fabrication and characterization of micro- and nanostructures in laser host materials, and laser-assisted thin-film deposition. Since 2003, he is a Researcher with the Centre National de la Recherche Scientifique (CNRS), XLIM Research Institute, University of Limoges, France. His current research activities are focused on the development of new materials for microelectronics and optics, RF-MEMS reliability, and optical switching using MEMS technology.

**Julien Givernaud** received the Bachelor degree in material science from the Engineering National School of Limoges (ENSIL), France, in 2006, and he is currently working for obtaining his Ph.D. at the University of Limoges. Since 2007, he is with the XLIM Research Institute, CNRS/University of Limoges. His research interests include the integration of smart materials (mainly $VO_2$) in RF microwave devices.

https://doi.org/10.1017/S175907871100095X Published online by Cambridge University Press

**Jean-Christophe Orlianges** received the Ph.D. degree in material sciences from the University of Limoges, Limoges, France, in 2003. From 2008 to 2009, he was with the "Centre National de la Recherche Scientifique" (CNRS), as a Research Engineer with XLIM Laboratory. He is currently an Assistant Professor with the Faculty of Science, University of Limoges. He conducts research with the "Sciences des Procédés Céramiques et de Traitements de Surface" (SPCTS) Laboratory, Unité Mixte de Recherche (UMR) 6638, CNRS/University of Limoges. His main research interests include pulsed-laser thin-films deposition techniques, nanostructured materials, development, and integration of new materials in electronic and optic devices.

**Corinne Champeaux** received the Ph.D. degree in electrical engineering from the University of Limoges, Limoges, France, in 1992. Since 1992, she has been an Assistant Professor with the Faculty of Science, University of Limoges. She currently conducts research with the Sciences des Procédés Céramiques et de Traitements de Surface (SPCTS) Laboratory, Unité Mixte de Recherche (UMR) 6638, Centre National de la Recherche Scientifique (CNRS), University of Limoges. Her main research interests are laser–matter interactions and pulsed-laser thin-films deposition techniques. She is involved with the development and fabrication of MEMS components through the elaboration of new materials and fabrication processes.

**Pierre Blondy** (M'00) received the Ph.D. and Habilitation degrees from the University of Limoges, Limoges, France, in 1998 and 2003, respectively. From 1998 to 2006, he was with the Centre National de la Recherche Scientifique (CNRS), as a Research Engineer with XLIM Laboratory, where he began research on RF-MEMS technology and applications to microwave circuits. He is currently a Professor at the University of Limoges, leading a research group on RF-MEMS. He was a visiting researcher at the University of Michigan, Ann Arbor, USA in 1997 and at the University of California at San Diego, La Jolla, USA in 2006 and 2008. Dr Blondy was an Associate Editor for the *IEEE Microwave and Wireless Components Letters* in 2006. He is a member of the IEEE International Microwave Conference Technical Program Committee since 2003.

https://doi.org/10.1017/S175907871100095X Published online by Cambridge University Press